THE JOURNAL OF BIOLOGICAL CHEMISTRY VOL. 284, NO. 20, pp. 13792–13803, May 15, 2009

Active Plasma Kallikrein Localizes to Mast Cells and Regulates Epithelial Cell Apoptosis, Adipocyte Differentiation, and Stromal Remodeling during Mammary Gland Involution*

Received for publication, January 22, 2009, and in revised form, March 16, 2009 Published, JBC Papers in Press, March 18, 2009, DOI 10.1074/jbc.M900508200

Jennifer N. Lilla[‡], **Ravi V. Joshi**[§], **Charles S. Craik**[§], **and Zena Werb**[‡1]

From the [‡]*Department of Anatomy, University of California, San Francisco, California 94143-0452 and the* [§]*Department of Pharmaceutical Chemistry, University of California, San Francisco, California 94143-2280*

The plasminogen cascade of serine proteases directs both development and tumorigenesis in the mammary gland. Plasminogen can be activated to plasmin by urokinase-type plasminogen activator (uPA), tissue-type plasminogen activator (tPA), and plasma kallikrein (PKal). The dominant plasminogen activator for mammary involution is PKal, a serine protease that participates in the contact activation system of blood coagulation. We observed that the prekallikrein gene (*Klkb1*) is expressed highly in the mammary gland during stromal remodeling periods including puberty and postlactational involution. We used a variant of ecotin (ecotin-PKal), a macromolecular inhibitor of serine proteases engineered to be highly specific for active PKal, to demonstrate that inhibition of PKal with ecotin-PKal delays alveolar apoptosis, adipocyte replenishment, and stromal remodeling in the involuting mammary gland, producing a phenotype resembling that resulting from plasminogen deficiency. Using biotinylated ecotin-PKal, we localized active PKal to connective tissue-type mast cells in the mammary gland. Taken together, these results implicate PKal as an effector of the plasminogen cascade during mammary development.

The plasminogen cascade of serine proteases regulates both development and tumorigenesis in the mammary gland (1, 2). The ultimate effector in this cascade, plasminogen as its active form, plasmin, is mediated by an intricate cascade of plasminogen activators and protease inhibitors. Plasminogen-deficient mice exhibit significant defects in lactational competence and post-lactational mammary gland involution (2), the process by which the differentiated, lactating gland remodels after the cessation of lactation to a state approaching that of the non-pregnant animal. The effect of plasminogen loss is exacerbated after a round of pregnancy and lactation: plasminogen-null mammary glands have poorly developed secretory alveoli during lactation, and upon involution, never fully involute. Instead, the secretory alveoli fail to regress normally. Moreover, the stroma becomes fibrotic and is cleared incompletely of partially degraded epithelial basement membrane. Because plasminogen-deficient mice largely are unable to support a second round of pregnancy and lactation (2), this suggests that the involution defect is not overcome by activities of other proteases eventually. These studies establish plasminogen as a crucial protease in normal mammary gland biology.

Plasminogen is synthesized in the liver and circulates as a zymogen through blood plasma to all vascularized tissues of the body. As this expression and circulation are constant, activation of the plasminogen cascade must be controlled locally to avoid rampant tissue proteolysis. Accordingly, plasminogen can be activated to plasmin by urokinase-type plasminogen activator (uPA),[2] tissue-type plasminogen activator (tPA), and plasma kallikrein (3). Though tPA and uPA are efficient and well characterized plasminogen activators, studies of mice singly as well as doubly targeted for deficiency of these plasminogen activators show they do not recapitulate the mammary gland phenotype of plasminogen deficiency (4). Instead, through use of variants of ecotin, a macromolecular inhibitor for serine proteases derived from *Escherichia coli*, we have previously suggested that the dominant plasminogen activator for mammary stromal involution is plasma kallikrein (PKal) (4).

PKal, the activated form of the zymogen prekallikrein encoded by the *Klkb1* gene, is an 80-kDa serine protease that also is synthesized in the liver and circulates in plasma at about 40–50 μg/ml. PKal participates in the contact activation system of intrinsic coagulation by activating high molecular weight kininogen into bradykinin (5–8). While plasma kallikrein is so-named due to its bradykinin-generating ability, it is in fact structurally and catalytically distinct from the large family of tissue kallikreins, which activate an alternate form of bradykinin from both high and low molecular weight kininogen (9). Moreover, PKal activates plasminogen into plasmin *in vitro* (3), albeit less efficiently than uPA and tPA.

To determine the role of PKal in plasminogen activation *in vivo* in mammary gland involution, we used a variant of ecotin that was engineered to be highly specific for active PKal (10). This ecotin variant, named ecotin-PKal, inhibits plasminogen activation *in vivo* in a model of wound healing (11). In this

* This work was supported, in whole or in part, by National Institutes of Health Grants CA057621 and CA072006 from the NCI. This work was also supported by a Predoctoral Fellowship from the Department of Defense DOD-CMDRP Breast Cancer Research Program (W81XW-05-0272) (to J. N. L.).

[1] To whom correspondence should be addressed: Dept. of Anatomy, HSW 1323, University of California, San Francisco, CA 94143-0452. Tel.: 415-476-4622; Fax: 415-476-4565; E-mail: zena.werb@ucsf.edu.

[2] The abbreviations used are: uPA, urokinase-type plasminogen activator; tPA, tissue-type plasminogen activator; PKal, plasma kallikrein; DPPI, dipeptidyl peptidase I; ECL, enhanced chemiluminescence; DAB, 3,3′-diaminobenzidine; RT-qPCR, real-time quantitative polymerase chain reaction; HPRT, hypoxanthine phosphoribosyltransferase; RQ, quantile regression; ECM, extracellular matrix; CAE, chloroacetate esterase; PBS, phosphate-buffered saline; DAPI, 4′,6-diamidino-2-phenylindole.

study, we demonstrate that inhibition of PKal significantly delays mammary gland involution.

EXPERIMENTAL PROCEDURES

Experimental Animals—Care of animals and all animal experiments were performed in accordance with protocols approved by the UCSF Institutional Animal Use and Care Committee (IACUC). For postlactational mammary gland involution studies, pregnant female CD1 mice (Charles River Laboratories) gave birth naturally, then offspring number was normalized to 8 per mouse for each experimental animal. Offspring were weaned after 10 days of lactation, which became day 0 of involution. On days 1–4 of involution, mice were injected intraperitoneally every 12 h with either normal saline or 100 μg of ecotin-PKal as previously described (4). Animals were sacrificed on day 5 of involution ($n = 8$/group) and mammary glands were harvested. Animals were also sacrificed on each of days 1–4 of involution or were treated for days 1–4 then allowed to recover until sacrifice on day 9 of involution ($n = 2$/time point).

For PKal localization experiments, wild-type FVB and CD1 mice were obtained from Charles River Laboratories. C57BL/6J-*Kit*$^{W\text{-}sh/W\text{-}sh}$ mice were obtained from the Jackson Laboratory and C57BL/6 mice were obtained from Charles River Laboratories. Dipeptidyl peptidase I (*DPPI* (−/−)) knock-out mice (12) were provided by Dr. Lisa Coussens (UCSF). For all mouse mammary models, thoracic mammary glands 2 and 3 were removed for RNA or protein collection, and/or abdominal mammary glands 4 were removed for microscopic analysis. To inhibit mast cell degranulation, CD1 female mice (Charles River Laboratories) were injected intraperitoneally with 50 mg/kg body weight sodium cromoglycate (Sigma) dissolved in saline as previously described (13), and then 2 h later, mammary glands were removed for analysis.

Preparation of Ecotin-PKal—A pTacTac expression vector containing the Ecotin-PKal gene was transformed into XL-1 blue (Stratagene, La Jolla, CA) competent *E. coli* and grown at 37 °C in 2xYT media with carbenicillin at 100 μg/ml to an $A_{600} = 0.4$. Isopropyl-β-D-thiogalactoside was added to 0.5 mM concentration and incubated overnight at 37 °C. The cell culture was harvested by centrifugation, and the cell pellet was resuspended in 25% sucrose 10 mM Tris-HCl, pH 8.0. The cell suspension was then treated for 2 h with lysozyme and EDTA at final concentrations of 1.5 mg/ml and 50 mM, respectively, to release the periplasmic protein content. The cell debris was pelleted, and the resulting supernatant was dialyzed against 1 mM HCl. The dialysate was again centrifuged to remove any precipitated material and then adjusted to pH > 7.0 with 1 M Tris, pH 8.0. NaCl was added to the supernatant to a final concentration of 300 mM and the solution was boiled in water at 100 °C for 10 min. Denatured material was removed by centrifugation, and the solution was dialyzed against distilled water overnight. The dialysate was concentrated to <5 ml by membrane ultrafiltration using Amicon YM-10, (Millipore, Billerica, MA) and then syringe-filtered (0.22 μM). Trifluoroacetic acid was added to 0.1% and Ecotin-PKal was purified from a C4 semi-prep column (Vydac, Deerfield, IL) using an acetonitrile gradient. Ecotin-PKal typically eluted at 35% acetonitrile, 0.1% trifluoroacetic acid water (v/v). Fractions corresponding to Ecotin-PKal were lyophilized, re-dissolved in distilled water, and stored at 4 °C for later use.

Ecotin-PKal Inhibition Kinetics—Active mouse plasmin was obtained from Haematologic Technologies Inc. (Essex Junction, VT). Recombinant mouse plasma kallikrein (R&D Systems, Minneapolis, MN) was obtained as a pro-enzyme and activated with thermolysin (R&D Systems) as described by the manufacturer. All binding titrations and dilutions of reagents were carried out in reaction buffer: 50 mM Tris pH 7.5, 150 mM NaCl, 0.005% Tween 20. Ecotin-PKal was diluted to final concentrations ranging from 1 nM to 100 μM for plasmin assays and from 0.1 pM to 10 μM for plasma kallikrein assays. In the binding assays, plasmin and plasma kallikrein were present at 10 nM and 1 nM, respectively. The reactions were performed in triplicate in a 96-well plate with a final volume of 250 μl. The reactants were incubated at 37 °C for 4 h. After the incubation time, the activity was measured by addition of a *p*-nitroanilide peptide substrate and then by monitoring the absorbance ($\lambda = 405$ nm) at room temperature. Plasmin activity was measured using the S-2251 substrate (Chromogenix, Milano, Italy) at a final concentration of 600 μM. Plasma kallikrein activity was measured using the S-2232 substrate (Chromogenix) at a final concentration of 800 μM. Initial velocities of the reaction were calculated using Softmax Pro Software (Molecular Devices, Sunnyvale, CA). The rates were averaged over all three trials. The average rates were normalized to the rate of the negative control (0 nM ecotin-PKal) sample to yield V/V_{max}. The rates were plotted *versus* ligand (ecotin-PKal) concentration and fitted to $V/V_{max} = 1 - L/(IC_{50} + L)$ using Kaleidograph (Synergy Software, Reading, PA) to determine the K_i for each of the enzymes.

Western Blotting and Affinity Chromatography—Mammary glands were lysed in pH 8 radioimmune precipitation assay buffer (50 mM Tris-HCl, pH 7.5, 150 mM NaCl, 1% Nonidet P-40, 0.5% deoxycholate, and 0.1% sodium dodecyl sulfate (SDS)) plus complete protease inhibitors, homogenized, then centrifuged at 14,000 rpm at 4 °C to collect supernatant. Ecotin-PKal biotinylated with Sulfo-NHS-LC-LC biotin (EZ-Link, Pierce) was used to generate affinity chromatography columns using immobilized streptavidin beads (Pierce). Mammary lysates (1 mg) were added to the columns and incubated for 2 h at 4 °C. PKal was detected by Western blotting of mammary lysates, column flow-thru, and column beads boiled in sample buffer. Samples were separated by electrophoresis under reducing, denaturing conditions on 4–12% bis-Tris acrylamide gels (Invitrogen, Carlsbad, CA) and then blotted onto polyvinylidene difluoride membranes (Amersham Biosciences, Piscataway, NJ). Membranes were blocked with 5% nonfat milk and 0.1% Tween in PBS and incubated overnight with a polyclonal antibody raised against recombinant mouse KLKB1 (1:1000, R&D Systems) in blocking solution. Membranes were washed and incubated with donkey anti-goat IgG (1:2000, Amersham Biosciences) before detection with ECL chemiluminescent reagent (Amersham Biosciences).

Histology, Immunohistochemistry, and Immunofluorescence—Right no. 4 mammary glands were removed, weighed, and immediately embedded in OCT (Sakura, Torrance, CA) medium on dry ice. Left no. 4 mammary glands were removed

and fixed overnight in 4% paraformaldehyde at 4 °C, then processed for paraffin embedding. 5-μm frozen or paraffin sections were cut for use in histology, enzyme histochemistry, immunohistochemistry, and immunofluorescence. To visualize gland lipid content, frozen sections were fixed additionally overnight in 4% paraformaldehyde, then rinsed in PBS, and air-dried for ≥3 h. Slides were then stained in Oil Red O (60% saturated Oil Red O (Sigma, 0.5% in isopropyl alcohol); 40% (1% type III corn dextrin (Sigma) in distilled water)) for 20 min. Slides were rinsed in PBS then counterstained briefly in Gill's hematoxylin (Sigma) and rinsed and stored in PBS. To examine overall gland morphology and stromal composition, Masson's Trichrome (Sigma) was used to stain paraffin sections according to the manufacturer's instructions. To visualize collagen content in the glands, paraffin sections were stained with 0.1% sirius red in saturated picric acid (picro-sirius red) (14) and observed under polarizing light. We identified apoptotic cells in paraffin sections of mammary tissue using an antibody against caspase-cleaved cytokeratin 18 (M30 CytoDEATH, Roche, Mannheim, Germany), a marker of cells undergoing apoptosis (15). Positively stained cells were visualized with mouse-on-mouse immunodetection (Vector Laboratories, Burlingame, CA) and 3,3′ diaminobenzidine (Fast DAB, Sigma).

To visualize mast cells, frozen sections were air-dried for ~30 min, post-fixed in ice-cold acetone for 10 min, rinsed in PBS, and then stained in either Toluidine blue (a metachromatic dye for mast cells, made up as 0.1% Toluidine blue O (Sigma) in 1% sodium chloride, pH 2.3), Csaba stain (Alcian blue/Safranin O, an amine/heparin stain for mast cells, made up as 0.36% Alcian blue (Sigma), 0.018% Safranin O (Sigma) in acetate buffer, pH 1.42), or by using an enzymatic reaction with naphthol AS-D chloroacetate esterase (Sigma) to detect chymase activity (16), then counterstained with Gill's hematoxylin or DAPI. For inhibitor-localization, frozen sections were prepared as above, then incubated overnight with 50 nM ecotin-PKal (10) biotinylated with Sulfo-NHS-LC-LC biotin (EZ-Link, Pierce), followed by 1-h incubation with Alexa 488-conjugated streptavidin (Invitrogen). Plasma kallikrein immunohistochemistry was performed on paraffin sections following sodium citrate antigen retrieval using a polyclonal antibody against recombinant mouse KLKB1 (R&D Systems) 1:50 overnight at 4 °C followed by a 30 min incubation with biotinylated anti-goat IgG secondary antibody (Amersham Biosciences) visualized using Vectastain ABC (Vector Laboratories) and 3,3′ diaminobenzidine (Fast DAB, Sigma).

Histological and immunochemical images were acquired at 100× or 200× using a Leica DMR microscope and Leica FireCam with accompanying software. Images were then imported into Adobe Photoshop software for analysis. Quantification of apoptotic cells was performed by counting the number of CytoDEATH$^+$ cells in lumen spaces per 100× field. Quantification of lipid content was performed by measuring the number of Oil red O$^+$ pixels per 100× field and expressing this as a percentage of the total field. Quantification of collagen was performed by measuring the number of collagen$^+$ pixels per 200× field and expressing this as a percentage of the total field. A minimum of 4 independent images per animal in each group was analyzed for each assay.

Real-time Quantitative Polymerase Chain Reaction—Total RNA was isolated from thoracic mammary glands cleared for muscle and lymph tissue at 3 weeks, 5 weeks, 15 days pregnant, 10 days lactating, and 4 days involuted CD1 mice. Liver tissue was used as a positive control. RNA isolation was performed using the RNA-Bee (Tel-Test, Inc., Friendswood, TX) phenol/guanidine thiocyanate/chloroform method for RNA isolation and concentration of RNA was measured spectrophotometrically. 5 μg of total RNA was used to perform reverse transcriptase polymerase chain reaction using Superscript II reverse transcriptase oligo(dT) reagents (Invitrogen). cDNA products were electrophoresed in 1% agarose/TAE gels to check thoroughness of the reverse transcriptase reaction.

Real-time quantitative polymerase chain reaction (RT-qPCR) was performed by the Biomolecular Resource Center at the University of California, San Francisco. *Klkb1* gene expression was normalized against expression of hypoxanthine phosphoribosyltransferase (HPRT), and reported as a RQ score relative to *Klkb1* expression in 5-week-old mammary glands. Oligonucleotide primers and TaqMan probe used were as follows: Klkb1 (1272): forward primer: 5′-TGGTCGCCAATGGGTACTG-3′; Klkb1 (1342): reverse primer: 5′-ATATACGCCACACATCTGGATAGG-3′; Klkb1 probe: 5′-(FAM)-CAGCTGCCCATTGCTTTGATGGAATT-(BHQ1)-3′.

PCR was conducted in triplicate with 20-μl reaction volumes of TaqMan Universal PCR Master Mix (Applied Biosystems), 0.9 mM of each primer, 250 nM probe, and 5 μl of cDNA. The PCR reaction was performed under the following conditions: 95 °C, 10 min, 1 cycle; 95 °C, 15 s then 60 °C, 2 min, 40 cycles. Analysis was carried out using the sequence detection software (SDS 2.1) supplied with TaqMan 7900HT (Applied Biosystems).

RESULTS

Ecotin-PKal Is Specific for Human and Mouse Plasma Kallikrein—Previous work conducted in this laboratory suggested that plasma kallikrein is a regulator of *in vivo* adipogenesis in the mammary gland during involution (4). However, the ecotin and ecotin variant (ecotin RR) used in the previous study target numerous serine proteases, including uPA in addition to PKal (17). Therefore, we used a recently developed variant of ecotin that has picomolar specificity for PKal (ecotin-PKal), while having K_i^* values four to seven orders of magnitude higher for related serine proteases. Importantly, the K_i^* of ecotin-PKal for human plasmin is six orders of magnitude higher than the K_i^* for human PKal, and seven orders of magnitude higher for the human plasminogen activators uPA and tPA (10). The only other protease that ecotin-PKal inhibits with reasonable (260-fold less) effectiveness is human Factor XIIa (10). This inhibition does not interfere with our investigation of the effects of PKal activity as PKal interacts with Factor XIIa as part of a reciprocal activation loop. Ecotin-PKal binding to serine proteases follows slow-tight binding kinetics (18).

To validate specificity in our mouse model system, binding titrations against mouse plasmin and mouse PKal were performed using ecotin-PKal as a ligand and measuring remaining (uninhibited) enzyme activity using *p*-nitroanilide substrates (Fig. 1*A*). The apparent affinities (K_i) of ecotin-PKal for mouse

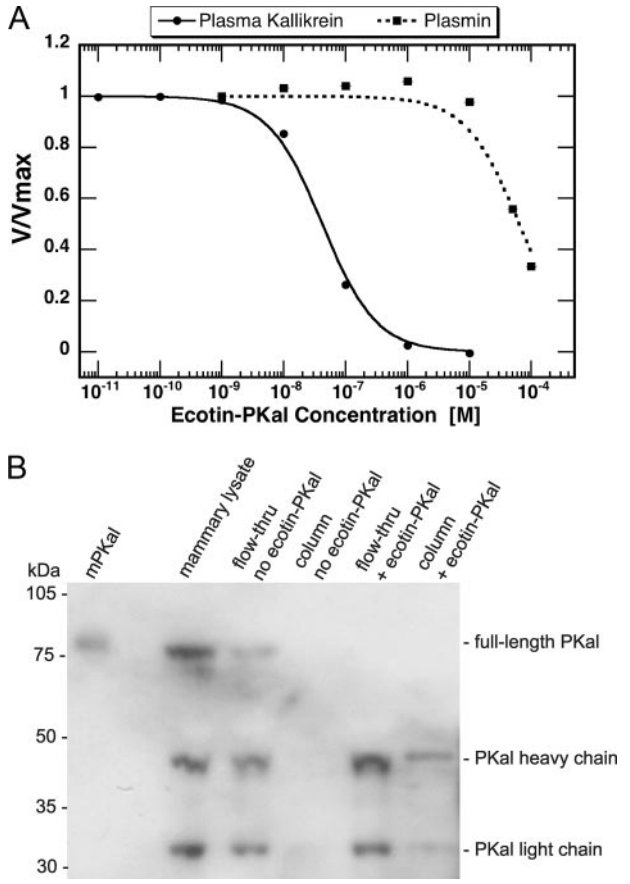

FIGURE 1. **Ecotin-PKal inhibits mouse plasma kallikrein and binds PKal isolated from mammary gland lysates.** *A*, binding assays were performed to determine K_i values for ecotin-PKal to mouse PKal or plasmin. After a 4-h incubation at 37 °C, remaining protease activity was measured using a *p*-nitroanilide substrate (see "Experimental Procedures"). Reaction velocities were averaged over three trials and normalized to the baseline reaction velocity. The apparent K_i of ecotin-PKal for mouse PKal was determined to be 40 nM; the K_i for mouse plasmin was determined to be 60 μM. *B*, protein lysates from 4-day-involuting mammary glands were run over either streptavidin-only beads (*no ecotin-PKal*) or streptavidin beads bound with biotinylated ecotin-PKal (+ *ecotin-PKal*). Flow-thru from the columns was collected, and bead-bound proteins were eluted by boiling the beads in sample buffer. All samples were subjected to electrophoresis and Western blotting using an antibody against mouse prekallikrein (α-mouse KLKB1, R&D Systems). The bands likely represent full-length PKal (~80 kDa), its heavy chain (42 kDa, unglycosylated), and its light chain (28 kDa, unglycosylated). *mPKal*, mouse prekallikrein peptide, R&D Systems), against which the antibody was raised.

PKal and mouse plasmin were determined to be 40 nM and 60 μM, respectively. The affinity of ecotin-PKal for mouse PKal is still 1000-fold greater than its affinity for mouse plasmin, although less than for human PKal. Therefore, to inhibit PKal *in vivo* during mammary gland involution, we estimated that in our dosing regimen, peak circulating concentrations of ecotin-PKal in mouse plasma approach 2 μM, nearly 30-fold less than the apparent K_i for ecotin-PKal inhibition of plasmin.[3] Thus, the effects of ecotin-PKal administration are due to the inhibition of mouse PKal and not of mouse plasmin in our model system.

We collected mammary glands from 4-day involuting mammary glands, when PKal is highly expressed in these tissues (see below), to determine whether ecotin-PKal can bind active PKal from mammary tissue lysate. Using biotinylated ecotin-PKal-bound streptavidin beads, we pulled down PKal from mammary gland lysates (Fig. 1*B*). The bands indicated on the blot represent the full-length protein (~80 kDa), and in its active form under reducing conditions, PKal heavy (~42 kDa) and light (~28 kDa) chains, which have at least one and two identified *N*-glycosylated Asn residues, respectively, according to the SwissProt Protein Data base. Similar results were obtained from 5-week-old virgin mammary gland lysates (data not shown). These data confirm that ecotin-PKal binds PKal found in the mammary gland.

Mouse Plasma Kallikrein Is Differentially Expressed in the Developing Mammary Gland—Prekallikrein (gene: *Klkb1*), the precursor of PKal, is expressed in a variety of mouse and human tissues outside of the liver (19–21). Accordingly, we wished to determine whether PKal is expressed in the mammary gland, and if its expression is altered during different phases of mammary gland development, when careful regulation of plasminogen activation is required.

The process of pubertal mammary gland development begins around 3 weeks of age and continues until the advancing ductal epithelium reaches the end of the fat pad, around 8–10 weeks of age. We examined *Klkb1* gene expression in the mouse mammary gland at different postnatal development time points (3 weeks, 5 weeks, 15 days pregnant, 10 days lactating, and 4 days involuting) by RT-qPCR. *Klkb1* mRNA was abundant during pubertal development, when the mammary gland is undergoing active remodeling as the ductal epithelium expands and advances through the stromal fat pad (Fig. 2*A*). During pregnancy and lactation, when the stroma has largely been replaced by secretory alveoli and extensive ductal structures, *Klkb1* mRNA was markedly reduced. *Klkb1* mRNA increased significantly during mammary gland involution, when the secretory epithelial structures die by apoptosis and the mammary stromal compartment is replenished. These findings indicate that PKal is produced in the mammary gland, and that its increased expression levels correlate with periods of stromal remodeling.

Biotinylated Ecotin-PKal Localizes Active Plasma Kallikrein to Mast Cells—Prekallikrein is expressed in the mammary gland in addition to circulating prekallikrein from the liver. However, it is active PKal that is inhibited by ecotin-PKal *in vivo*, resulting in repressed mammary gland involution. Therefore, we wished to identify which cells in the mammary gland are the sites of PKal activity. We used the biotinylated form of ecotin-PKal to localize the active protease in 5-day-involuting mammary gland tissue sections, taking advantage of ecotin-PKal's high affinity for the active form of PKal. Biotinylated ecotin-PKal stained a subset of cells in the mammary gland (Fig. 2*B*), and this staining was absent in the presence of a 1000-fold excess of non-biotinylated ecotin-PKal (Fig. 2*C*). The ecotin-PKal-positive cells were clustered near blood vessels, ducts, and scattered throughout the fatty stroma and the loose connective tissue surrounding the mammary fat pad (Fig. 2*D*). We identified these active $PKal^+$ cells as mast cells, as shown by Csaba staining of serial tissue sections (Fig. 2*E*). We confirmed that PKal localizes to mammary gland mast cells by direct immunohistochemical staining for PKal using a polyclonal antibody against mouse KLKB1, followed by counterstaining with Tolu-

[3] C. Craik, unpublished data.

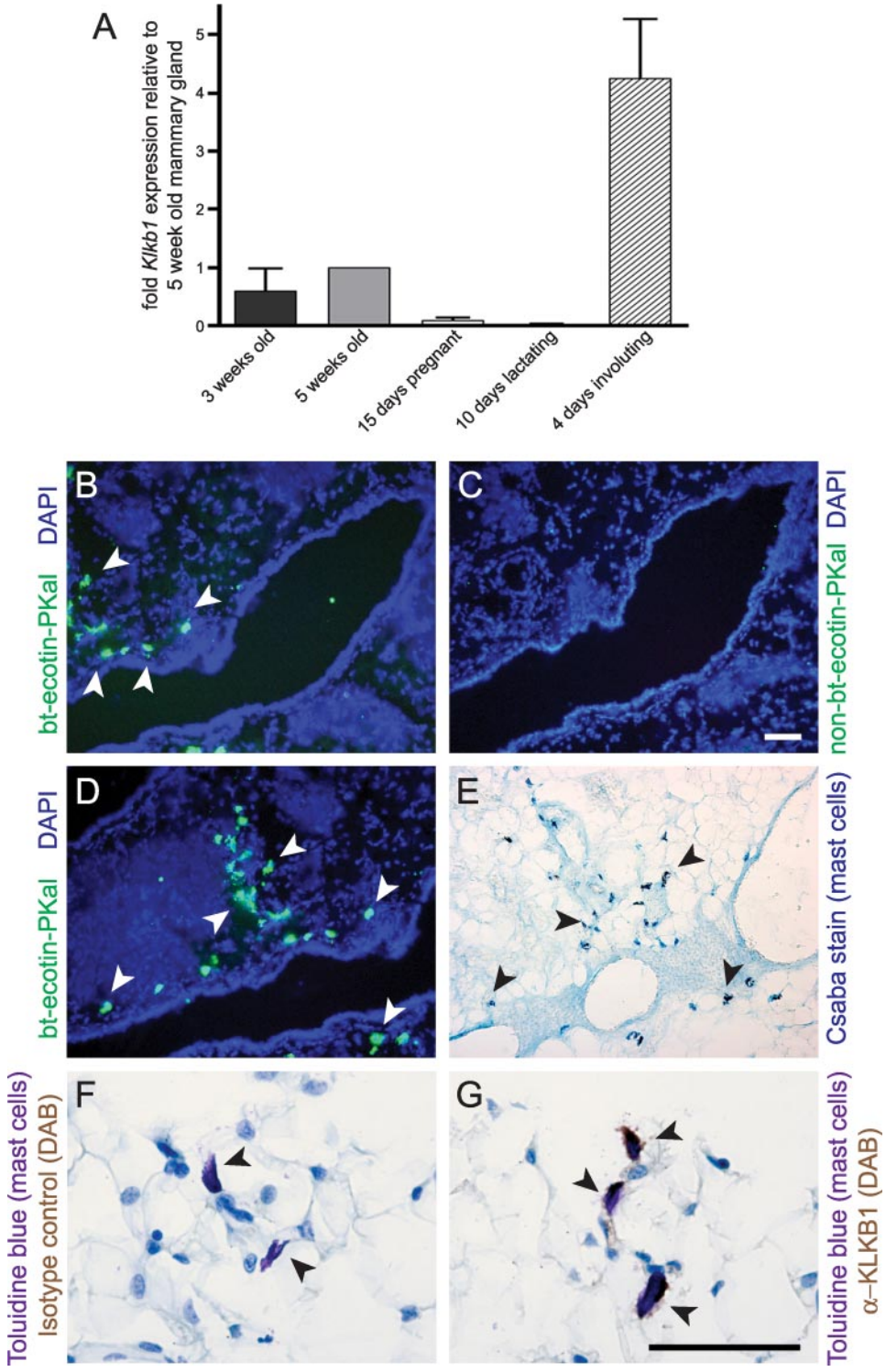

FIGURE 2. **Plasma kallikrein message is present in the mammary gland and the active protease localizes to mammary gland mast cells.** *A*, real-time qPCR analysis of *Klkb1* expression in mammary gland RNA shows that *Klkb1* is differentially expressed throughout postnatal mammary gland development. RT-qPCR performed in triplicate for *Klkb1* expression normalized against HPRT and reported as a RQ score relative to *Klkb1* expression in 5-week-old mammary glands from CD1 mice. Increased expression correlates to periods of active stromal remodeling during mammary development. *Error bars* represent S.D. *B*, frozen section of 5-day-involuting mammary gland using Alexa 488-conjugated streptavidin (*green*) to visualize 50 nM bound biotinylated ecotin-PKal; DAPI counterstain (*blue*). *White arrowheads* indicate representative ecotin-PKal staining. *C*, staining is absent in presence of excess (50 μM) non-biotinylated ecotin-PKal. *Scale bar* for *B–E* is 100 μm. *D*, mast cells clustered around a large mammary blood vessel stain positively for active PKal when visualized using biotinylated ecotin-PKal. Frozen sections of 5-day-involuting mammary gland were stained with biotinylated ecotin-PKal as above. *E*, serial section of *D* stained for mast cells with Csaba stain shows that cells labeled by ecotin-PKal are mast cells. *Black arrowheads* indicate representative Csaba stained-mast cells. *F*, paraffin section of 5-week-old mammary gland shows mast cells in the mammary stroma stained with Toluidine blue, which stains mast cell granules purple. Sections were treated as a negative control for staining shown in *G*. *Black arrowheads* indicate Toluidine blue-stained mast cells. *G*, serial section of *F* immunostained with KLKB1 antibody followed by DAB shows that mammary gland mast cells stain positively for plasma kallikrein using conventional immunohistochemistry. *Black arrowheads* indicate Toluidine blue-stained, DAB+ mast cells. *Scale bar* for *F* and *G* is 100 μm.

idine blue, another mast cell-specific stain (Fig. 2, *F* and *G*). These data represent a novel connection between active plasma kallikrein and mast cells.

Mast cells in both mice and humans can be subdivided into two general classes, connective tissue and mucosal, according to tissue of origin, staining properties, proteoglycan and protease content, and histamine concentration (22). Connective tissue-type mast cells are predominantly found in skin and the peritoneal cavity, while mucosal-type mast cells are found in the lamina propria of the small intestine and in the lung. Because PKal localization to mast cells has not previously been demonstrated, we tested the ability of ecotin-PKal to localize the active protease to different mast cell types in other tissues. We found that ecotin-PKal-stained connective tissue-type mast cells of the skin and tongue (Fig. 3, *A* and *B*), but not the mucosal-type mast cells of the intestine (Fig. 3*D*). Importantly, we also did not see ecotin-PKal staining in the liver (Fig. 3*C*), where prekallikrein is produced for circulation in the plasma, thus demonstrating the specificity of the inhibitor for the active form of the protease.

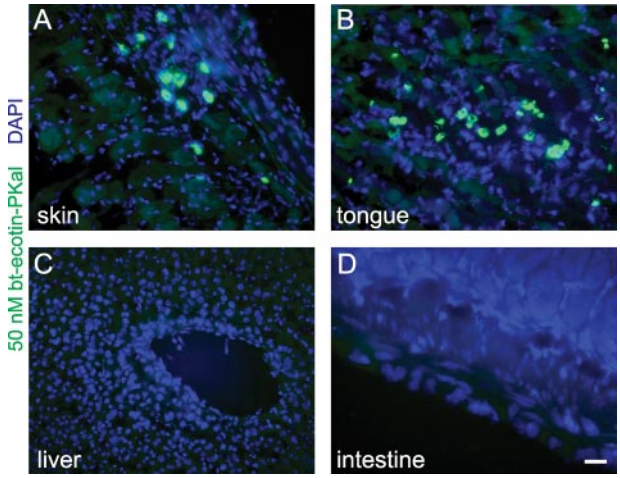

FIGURE 3. **Biotinylated ecotin-PKal stains tissues with connective tissue-type mast cells but not liver.** Frozen sections using 50 nM ecotin-PKal plus Alexa 488-conjugated streptavidin, DAPI counterstain. *Scale bar* for *A–D* is 100 μm. Active PKal is seen in mast cells of the skin (*A*) and tongue (*B*), but not in liver (*C*) or intestine (*D*). Active PKal cannot be seen in liver, where prekallikrein is synthesized but not activated, and therefore is not bound by ecotin-PKal. Active PKal is not seen in the small intestine, where mast cells are of the mucosal subtype.

Plasma Kallikrein Specifically Localizes to Mast Cell Granules—To determine the subcellular localization of ecotin-PKal in mast cells, we co-stained cells for chymase activity using naphthol chloroacetate esterase, a marker of mast cell granule chymase that appears red in both brightfield and fluorescent microscopy (16). PKal localized to the cytoplasmic granules of mast cells in wild-type mice (Fig. 4*A*). Ecotin-PKal staining was absent in mammary glands of mast cell-deficient *Kit* mutant W-*sash* mice (23), supporting the observation that active PKal is only seen in mast cells in the mammary gland (Fig. 4*B*). By confocal microscopy, we pinpointed the subcellular localization of active PKal to mast cell granules (Fig. 4*C*). However, not all granules stained positively for ecotin-PKal within a specific mast cell, and ~10% of observed mammary mast cells were not positive for active PKal (data not shown). These observations suggest that PKal-mast cell interactions are context-specific, though the mechanisms for this interaction still need to be identified.

We then asked whether the localization of PKal to mast cell granules depended on the activation state of the mast cell by stabilizing mast cells or by using mutant mice that have a defect in activating their mast cell serine proteases. To stabilize mast cells from degranulation, we used cromolyn sodium, which is thought to inhibit the calcium ion influx that is required to trigger mast cell degranulation (24). Dipeptidyl peptidase I (DPPI, or cathepsin C)-deficient mice have mast cells that can degranulate, yet their mast cell proteases are either inactive or down-regulated (25). We compared ecotin-PKal/chloroacetate esterase staining in mammary gland mast cells in wild-type, mast cell-stabilized, and mast cell protease-inactivated mice. In normal, wild-type adult virgin mice, ecotin-PKal localized specifically to mast cell granules (Fig. 4*D*). In mice treated with cromolyn sodium, active PKal localization changed to a "halo" surrounding the mast cells in the majority of cells observed (Fig. 4*E*). Mammary mast cells from DPPI-

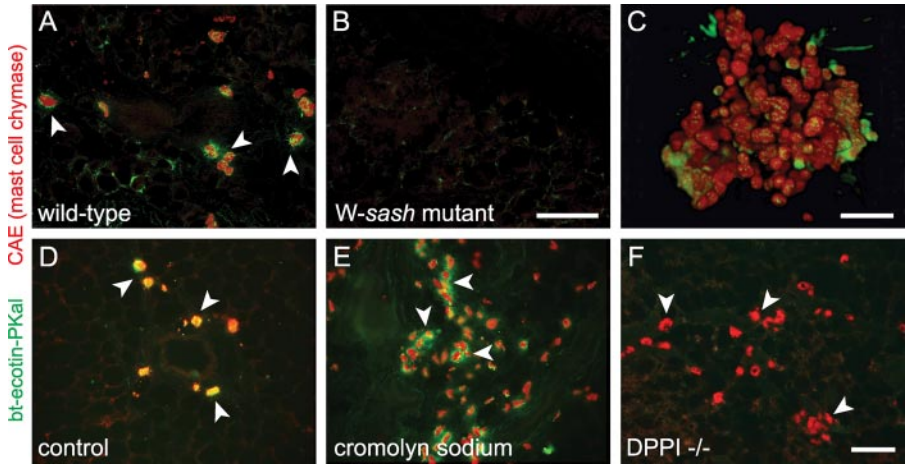

FIGURE 4. **Ecotin-PKal stains mast cell granules, and colocalization is dependent on the activation of mammary mast cells.** *A*, biotinylated ecotin PKal colocalizes specifically with mast cell granules. Frozen section of 5-week-old wild-type mammary gland using 50 nM biotinylated ecotin-PKal plus Alexa 488-conjugated streptavidin (*green*) and naphthol chloroacetate esterase (*CAE*), a marker of mast cell granule chymase (*red*). *White arrowheads* indicate representative co-labeled mast cells. *B*, frozen section of 5-week-old W-sash mutant mouse mammary gland, which is deficient for mast cells, stained with biotinylated ecotin-PKal and CAE as above. *Scale bar* for *A* and *B* is 100 μm. *C*, confocal image of a single mast cell from a 5-week-old mouse mammary gland stained with biotinylated ecotin-PKal and CAE as described above. Not all granules are ecotin-PKal-positive, and not all mammary mast cells are stained by ecotin-PKal (data not shown). *Scale bar* is 10 μm. *D–F*, adult virgin mammary gland frozen sections stained with 50 nM biotinylated ecotin-PKal and CAE. *White arrowheads* indicate representative mast cells. *D*, wild-type, saline controls show PKal localized to mast cell granules. *E*, PKal stains as a "halo" around mast cells in wild-type mice treated with cromolyn sodium, which stabilizes mast cells from degranulating. *F*, mammary glands from mice deficient for cathepsin C (*DPPI*), the activator of most mast cell granule proteases, do not stain positively for PKal. *Scale bar* for *D–F* is 100 μm.

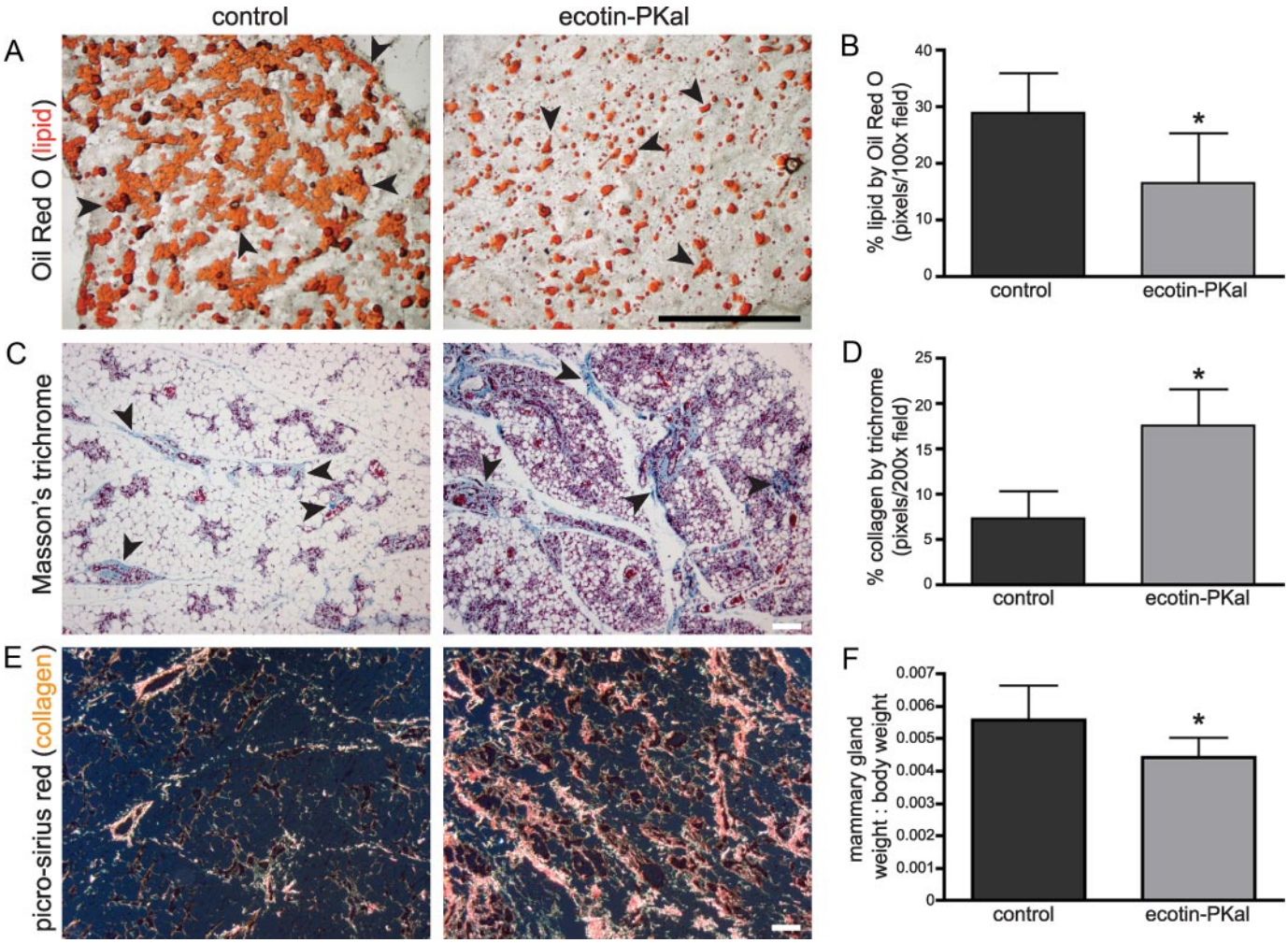

FIGURE 5. **Delay in mammary gland involution after treatment with ecotin-PKal.** Animals were treated twice daily during the first 4 days of involution with 100 μg of ecotin-PKal or with vehicle control. $n = 8$ mice/group. All error bars represent S.D. *A*, frozen sections of mammary glands stained with Oil Red O for lipid show ecotin-PKal-treated glands have fewer and less mature adipocytes. *Black arrowheads* indicate representative lipid staining. *Scale bar* is 1 mm. *B*, quantification of lipid content by Oil Red O staining shows ecotin-PKal-treated glands have significantly less lipid after 4 days of involution. Student's *t* test: $p = 0.041$. *C*, paraffin sections of mammary glands stained with Masson's trichrome to detect collagen (*blue*) and cytoplasm (*pink*) show that ecotin-PKal-treated glands have more collagen deposition and more immature stromal cells than controls. *Black arrowheads* indicate representative areas of collagen deposition. *Scale bar* is 100 μm. *D*, quantification of collagen content by Masson's trichrome stain shows ecotin-PKal-treated glands have significantly more collagen. Student's *t* test: $p = 0.003$. All error bars represent S.D. *E*, paraffin sections of mammary glands stained with picro-sirius red to demonstrate by birefringence under polarized light the difference between thick (*orange-yellow*) and thin (*green*) collagen fibrils. Scale bar is 100 μm. *F*, abdominal mammary gland weights expressed as a ratio of overall body weight on day 5 of involution show that ecotin-PKal-treated glands weigh less after treatment than controls. Student's *t* test: $p = 0.029$.

deficient mice did not stain for active PKal (Fig. 4*F*), suggesting that DPPI activity is upstream of PKal activation. These changes in active PKal location relative to mast cell activity and mast cell protease activation suggest a potential interaction between plasma kallikrein activation and mammary gland mast cells.

Inhibition of Plasma Kallikrein Delays Mammary Gland Stromal Involution—We then determined the role of PKal in mammary gland involution. Mammary gland involution is a two-step process: first, the milk-producing alveolar cells apoptose, then the mammary gland undergoes a protease-dependent wave of matrix remodeling which allows the repopulation of the mammary stroma by unilocular adipocytes (26, 27). To determine the physiological function of PKal during mammary gland involution, we treated mice for the first 4 days of involution after pup weaning (days 1–4 of involution) with either ecotin-PKal or vehicle control (normal saline). On the fifth day, mammary glands were harvested and assessed by multiple means for markers of involution.

As extracellular matrix (ECM) remodeling is a key regulator of the adipocyte maturation process, allowing the cell shape changes that turn on pro-adipogenic transcription factors in differentiating adipocytes (28–30), insufficient remodeling of the mammary gland stroma during involution would delay return of an adipocyte-rich mammary fat pad. On day 5 of involution, ecotin-PKal-treated animals had significantly reduced mammary gland lipid, and morphologically fewer and less mature adipocytes in the involuted stroma (Fig. 5, *A* and *B*). Staining of ecotin-PKal-treated mammary glands for lipid showed that PKal is required for sufficient ECM remodeling to promote the regeneration of mature, lipid-filled adipocytes to the mammary gland stroma.

We next visualized stromal ECM deposition in ecotin-PKal-treated glands. We confirmed that the mammary glands did not

undergo normal ECM remodeling associated with involution. The ecotin-PKal-treated glands had significantly increased deposition of collagen around poorly involuted epithelial structures, along with immature, cytoplasm-rich stromal cells, indicating decreased lipid accumulation (Fig. 5, *C* and *D*). We then used picro-sirius red, which stains fibrillar collagen, to examine the location of collagen deposition. Under polarized light fibrillar collagen is birefringent and thick and thin collagen fibers can be distinguished (14). In control glands, thick collagen fibrils were seen rarely throughout the stroma, surrounding epithelial areas and large blood vessels, while thin collagen fibrils were scattered throughout the stroma (Fig. 5*E*). However, in ecotin-PKal-treated glands, thick collagen fibrils were abundant, with thin collagen fibrils only appearing in areas with mature adipocytes (Fig. 5*E*). These data suggest that PKal promotes adipocyte maturation and lipid replenishment in the mammary gland during involution and that this is related to collagen remodeling as the secretory epithelium regresses. This reduction in lipid replenishment was grossly evident in a comparison of mammary gland weights, which were significantly reduced in ecotin-PKal-treated glands as compared with controls (Fig. 5*F*). Thus, without PKal activity, the preadipocytes have a reduced ability to return to their mature round, unilocular lipid-filled shape, and collagen deposition takes place instead. Overall, these results demonstrate that inhibition of PKal for the first 4 days of mammary gland involution severely inhibits the stromal remodeling that is required for proper lipid replenishment of the post-lactational mammary gland.

Plasma Kallikrein Promotes Epithelial Apoptosis in the First Phase of Mammary Gland Involution—The primary phase of alveolar regression is accomplished through epithelial apoptosis, in which differentiated lobuloalveolar epithelial cells die without remodeling in the surrounding stroma. This is followed by the secondary, remodeling phase of mammary gland involution (27, 31). We examined ecotin-PKal-treated mammary glands in early involution for alterations in epithelial cell death that could delay or inhibit subsequent remodeling. We stained mammary glands on days 1 through 3 of ecotin-PKal treatment for caspase-cleaved cytokeratin 18 as a marker of epithelial cell apoptosis (15). On day 1 of involution, few cells were apoptotic, but by day 2, control glands had high numbers of apoptotic alveolar epithelial cells while ecotin-PKal-treated glands remained unchanged (Fig. 6, *A* and *B*). By day 3 of involution, ecotin-PKal-treated glands began to show increased yet still significantly fewer apoptotic cells (Fig. 6, *A* and *B*), suggesting that other mechanisms eventually overcome the effect of PKal inhibition on epithelial apoptosis. By day 4 of involution, most alveolar structures had collapsed and stromal remodeling was fully underway in control glands, while ecotin-PKal-treated glands were more heterogeneous, with some areas undergoing apoptosis, some areas beginning to undergo stromal remodeling, and some areas consisting of barely changed alveoli (data not shown). These time course data indicate that the delay in stromal remodeling observed at day 5 of involution is due to delays in secretory epithelial apoptosis observed in the first phase of involution caused by PKal inhibition. Taken together, we conclude that PKal activity plays a significant role in epithelial apoptosis in mammary gland involution.

Inhibition of Plasma Kallikrein Alters Epithelial-Stromal Balance during the Two Phases of Mammary Gland Involution—Our data indicate that PKal activity regulates both secretory epithelial apoptosis in the first phase of involution and subsequent stromal remodeling and lipid replenishment in the second phase. To obtain macroscopic evidence of this effect of PKal, we compared mammary gland weights of ecotin-PKal-treated glands to controls throughout the treatment period. Ecotin-PKal-treated glands initially weighed more than controls, representing a delay in secretory alveolar collapse; once apoptosis began in treated glands, they began to weigh less than control counterparts, representing a delay in adipocyte maturation and lipid replenishment (Fig. 7*B*).

We then treated mice with ecotin-PKal from days 1–4 of involution and allowed them to recover for 5 days. We found that the early differences under the influence of ecotin-PKal observed in mammary weights (Fig. 7*B*) and lipid staining (Fig. 7, *A* and *C*) were not fully relieved by day 9 of involution after a 5-day recovery period. Therefore, though inhibition of PKal is reversible, the return of PKal activity is not sufficient for the completion of the mammary gland involution process in a timely manner.

DISCUSSION

In this study we have shown that plasma kallikrein is a critical regulator of mammary gland involution, and that its activity is required both for secretory epithelial apoptosis and for stromal ECM remodeling and adipocyte replenishment. Overall, inhibition of PKal results in an arrested involution similar to that of the plasminogen-deficient mouse.

We observed that PKal had an effect on the first, apoptotic stage of mammary gland involution. Inhibition of PKal activity caused a 2–3-day delay in epithelial apoptosis, resulting in an overall delay in mammary gland involution. However, PKal clearly was not solely responsible for apoptosis during involution, since by day 3 of involution the PKal-inhibited glands began to undergo apoptosis at approximately half the rate of controls. Therefore it is likely that under conditions of systemic PKal inhibition with ecotin-PKal, the availability of other plasminogen activators dictates epithelial apoptosis. Interestingly, tPA and uPA expression increases in the second, remodeling phase of involution (27). In combination with the lack of phenotype in the *tPA; uPA* double-null mice, this suggests that PKal activation of plasminogen is required especially in the early phase of involution because it is the only plasminogen activator available (Fig. 8).

Our data indicate that PKal is necessary for the mammary gland stromal remodeling and adipocyte replenishment that are the hallmarks of the second phase of mammary involution. Without PKal activation of plasminogen, the collagen-rich mammary stroma cannot be remodeled to induce the return of mature adipocytes, which require the removal of the fibrotic ECM to upregulate lipogenic genes and deposition of a new basement membrane (28, 29). In keeping with this scenario, PKal-inhibited mammary glands had more collagen and fewer and less-mature adipocytes. Even after 5 days of recovery from PKal inhibition the mammary glands had not fully involuted.

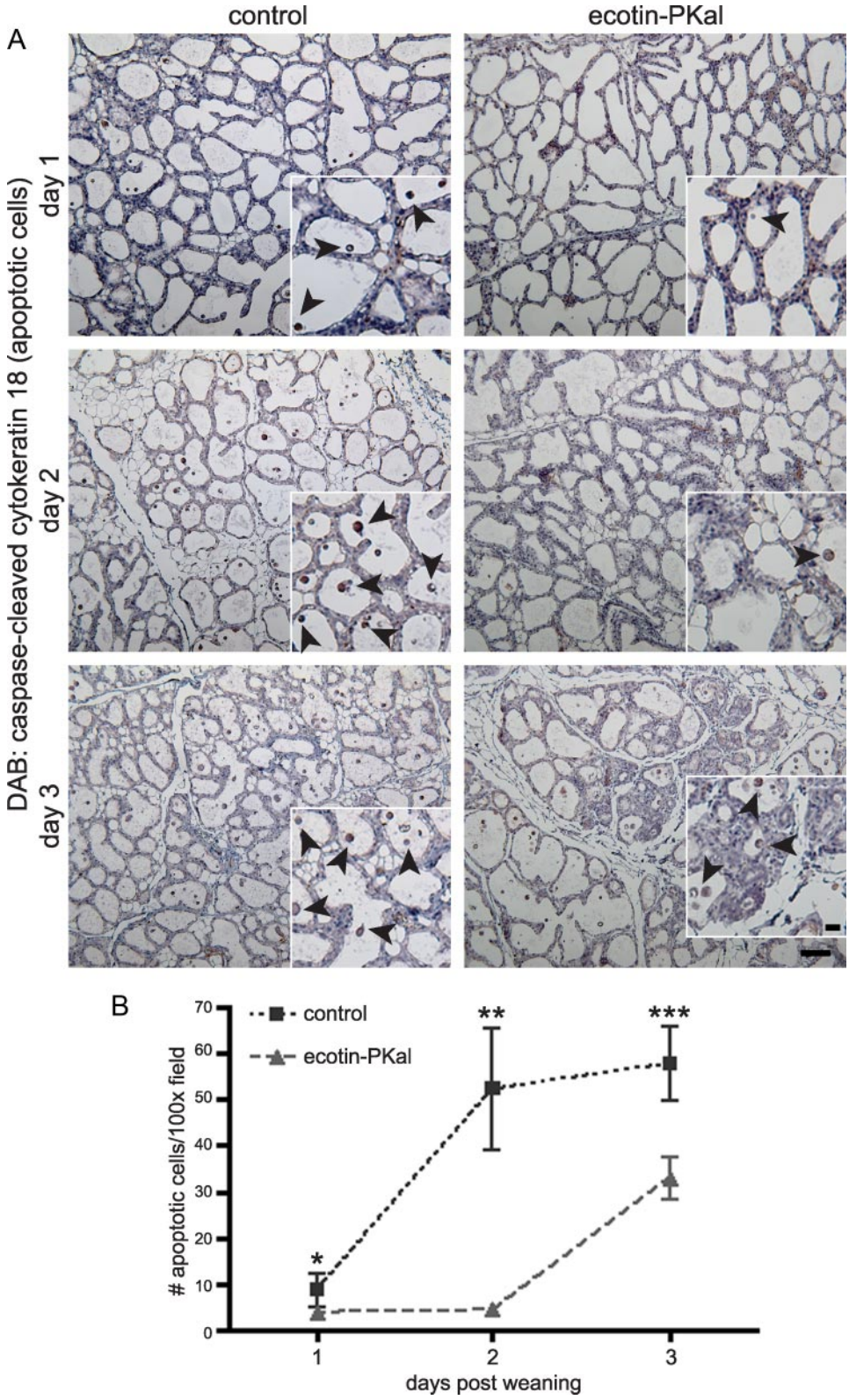

FIGURE 6. **Epithelial apoptosis is significantly delayed in ecotin-PKal-treated involuting mammary glands.** Animals were treated as described, $n = 2$ mice/group/time point. *A*, immunostaining of paraffin sections of involuting mammary glands from the first 3 days of treatment with an antibody against caspase-cleaved cytokeratin 18 (CytoDEATH) as a marker of early apoptosis. CytoDEATH$^+$ cells are stained brown (DAB). *Scale bar* is 100 μm. *Black arrowheads* indicate examples of detached apoptotic cells in insets. *Scale bar* for insets is 50 μm. *B*, quantification of apoptotic cells shows ecotin-PKal-treated mammary glands have a delay in epithelial cell apoptosis in the first 3 days of involution. Detached, CytoDEATH$^+$ cells in the lumens of involuting alveoli were counted per high power field. At least 5 images were counted per mouse per time point. Student's t tests: *, $p = 0.042$; **, $p = 1.88 \times 10^{-4}$; ***, $p = 0.01$. Error bars represent S.D.

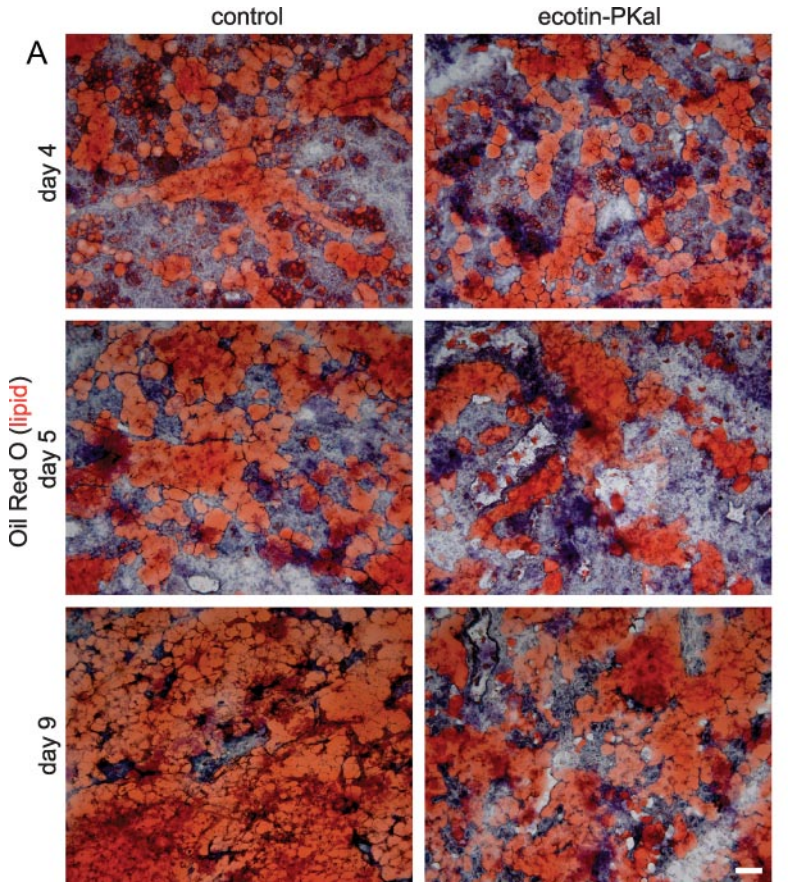

B

means of mammary gland weights:body weights (n=2/group/timepoint)

	day	control	ecotin-PKal
treatment period	0	0.035	0.035
	1	0.024	0.033
	2	0.021	0.027
	3	0.013	0.009
	4	0.010	0.010
	5	0.009	0.007
	9	0.007	0.005

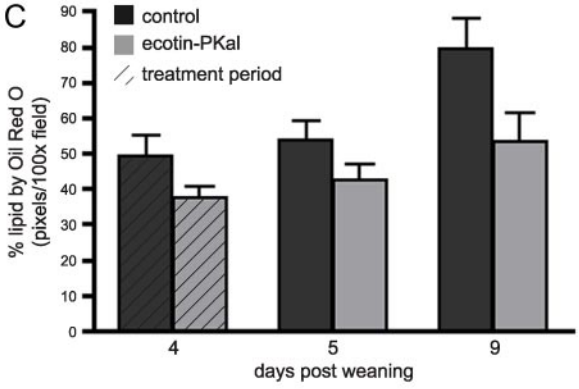

FIGURE 7. **Ecotin-PKal-treated mammary glands have an altered epithelial-stromal ratio during treatment.** Animals were treated as described, $n = 2$ mice/group/time point. *A*, frozen sections of mammary glands stained with Oil Red O for lipid show ecotin-PKal-treated glands have fewer and less mature adipocytes in the second phase of involution, even 5 days after end of treatment. *Scale bar* is 100 μm. *B*, ecotin-PKal-treated mammary glands weigh more during the first apoptotic phase of involution, then weigh less during the stromal remodeling phase. Abdominal mammary gland weights are expressed as a ratio of overall body weight on days 1–5 and day 9 of involution. Ecotin-PKal treatment occurred during days 1–5. *C*, quantification of lipid content by Oil Red O staining shows ecotin-PKal-treated glands have less lipid even after 5 days of recovery from ecotin-PKal treatment. *Shaded area* marks ecotin-PKal treatment. Error bars represent S.D.

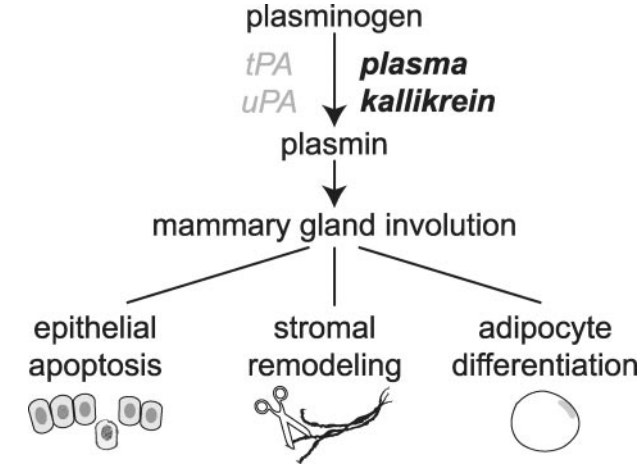

FIGURE 8. **Model of the function of plasma kallikrein during mammary gland involution.** As loss of tPA and uPA (in *gray*) does not recapitulate the effect of plasminogen deficiency in mammary gland involution, we posit that plasma kallikrein (in *bold*) is the critical activator of plasminogen during this process. Active PKal is required for apoptosis of the secretory epithelium, subsequent stromal remodeling, and eventual adipocyte replenishment of the mammary gland.

Although PKal has a little fibrinolytic activity of its own (11), its main ECM proteolytic function is thought to be in the activation of plasminogen either directly or through activation of pro-uPA (8) and perhaps pro-tPA (32), depending on the local context. Even though *tPA*-null, *uPA*-null, and *tPA; uPA* double-null mice have no mammary gland involution phenotype (4), it is not clear whether PKal alone can account for plasmin levels in these plasminogen activator-deficient glands that would be necessary for them to avoid the phenotype of plasminogen-deficient mice. However, recent evidence supports this possibility in the plasmin-dependent process of skin wound healing, where only *tPA; uPA* double-null mice treated with ecotin-PKal resulted in impairment comparable to that of plasminogen-deficient wound healing (11). Future studies in which *tPA; uPA* double-null mice are treated with ecotin-PKal during mammary involution could help confirm whether PKal, not tPA or uPA, is the primary activator of plasminogen in mammary gland involution.

It is also possible that the mechanism for PKal effect on mammary epithelial apoptosis during involution is not exclusively plasminogen-dependent. PKal's other, better-known role, as the activator of bradykinin through its release via proteolysis of high molecular weight kininogen, may also contribute to involution through the bradykinin effect on blood pressure, nitric oxide formation, and/or angiogenesis (33). To separate these two avenues of PKal activity, further use of ecotin-PKal in studies of the intrinsic coagulation cascade, as well as development of tools such as the PKal-deficient mouse,

could help elucidate the targets of PKal during mammary gland involution.

Our study also identified new patterns of expression and activation for plasma kallikrein. We detected *Klkb1* mRNA in the mammary gland, and determined that it is up-regulated in the gland during pubertal development and postlactational involution. Recent studies on the human prekallikrein promoter suggest that the promoter region has both repression and enhancer regions, as well as multiple alternative transcription initiation sites (34), providing multiple means for tissue-specific control of PKal transcription. It is interesting to speculate as to why PKal would be produced locally in tissues that would already potentially have a large reservoir of prekallikrein available through their vasculature. One hypothesis is that the source of PKal determines its substrate(s), either by bioavailability or by method of activation. Further studies to determine the tissue-specific regulation of PKal transcription could help establish whether systemic or local expression of this plasminogen activator is more important to the function of PKal during physiological processes such as mammary gland involution.

We took advantage of the development of ecotin-PKal to pinpoint the site of active PKal in the mammary gland. Surprisingly, using biotinylated ecotin-PKal as a probe for the active protease, we localized PKal in mammary gland and other tissues to connective tissue-type mast cells. While this result is intriguing, it poses an experimental difficulty in that connective tissue-type mast cells are not easily isolated from tissues, and differentiation of primary bone marrow cells into mast cells with interleukin-3 results in less mature mast cells of the mucosal phenotype (35), which were not positive for ecotin-PKal.

Furthermore, localization of PKal to mast cell granules was dependent on the activation state of the mast cells. Stabilizing mast cells through treatment with cromolyn sodium changed the localization of PKal so that mast cell granules were no longer PKal-positive, but instead active PKal was pericellular. One potential explanation for this observation is that cromolyn sodium may block endocytic pathways that would allow uptake of active PKal into mast cells, which may serve to sequester PKal from the extracellular environment. Alternatively, if mast cells are a source of prekallikrein production in the mammary gland, they may be able to activate and/or release PKal through exocytic pathways independent of mast cell granules. However, these hypotheses are complicated by our observation that active PKal was not detected in DPPI-deficient mammary gland mast cells. DPPI-deficient mast cells have reduced activation and/or expression of granule-associated proteases (12, 25), and thus mast cell protease activity may be required for PKal activation and/or sequestration to mast cell granules. In either case, these results identify a new pathway for plasma kallikrein activity and activation that has not been associated with mast cell granules previously and point to the need for further studies on the role of mast cells in mammary gland development.

In summary, we observed that PKal is the predominant plasminogen activator in the mammary gland during involution, and that PKal is locally expressed in the mammary gland and the active protease localizes to mast cell granules. This study establishes a plausible relationship between mast cells, PKal, and plasmin conversion in the mammary gland that represents a novel pathway for the plasminogen activation cascade. Given the diverse functions of plasmin in physiological processes including fibrinolysis, wound healing, and activation of the complement system, it is important to better understand how plasminogen is specifically activated by upstream factors, and how those factors may be selectively inhibited to mediate plasmin activity better in pathological and therapeutic processes.

Acknowledgments—We thank A. Allart Stoop and Dinlaka Sriprapundh for providing ecotin-PKal.

REFERENCES

1. Dano, K., Behrendt, N., Hoyer-Hansen, G., Johnsen, M., Lund, L. R., Ploug, M., and Romer, J. (2005) *Thromb. Haemost.* **93,** 676–681
2. Lund, L. R., Bjorn, S. F., Sternlicht, M. D., Nielsen, B. S., Solberg, H., Usher, P. A., Osterby, R., Christensen, I. J., Stephens, R. W., Bugge, T. H., Dano, K., and Werb, Z. (2000) *Development* **127,** 4481–4492
3. Miles, L. A., Greengard, J. S., and Griffin, J. H. (1983) *Thromb. Res.* **29,** 407–417
4. Selvarajan, S., Lund, L. R., Takeuchi, T., Craik, C. S., and Werb, Z. (2001) *Nat. Cell Biol.* **3,** 267–275
5. Baumgarten, C. R., Nichols, R. C., Naclerio, R. M., Lichtenstein, L. M., Norman, P. S., and Proud, D. (1986) *J. Immunol.* **137,** 977–982
6. Motta, G., Rojkjaer, R., Hasan, A. A., Cines, D. B., and Schmaier, A. H. (1998) *Blood* **91,** 516–528
7. Rojkjaer, R., and Schmaier, A. H. (1999) *Immunopharmacology* **43,** 109–114
8. Schmaier, A. H., Rojkjaer, R., and Shariat-Madar, Z. (1999) *Thromb. Haemost* **82,** 226–233
9. Lima, A. R., Alves, F. M., Angelo, P. F., Andrade, D., Blaber, S. I., Blaber, M., Juliano, L., and Juliano, M. A. (2008) *Biol. Chem.* **389,** 1487–1494
10. Stoop, A. A., and Craik, C. S. (2003) *Nat. Biotechnol.* **21,** 1063–1068
11. Lund, L. R., Green, K. A., Stoop, A. A., Ploug, M., Almholt, K., Lilla, J., Nielsen, B. S., Christensen, I. J., Craik, C. S., Werb, Z., Dano, K., and Romer, J. (2006) *EMBO J.* **25,** 2686–2697
12. Pham, C. T., and Ley, T. J. (1999) *Proc. Natl. Acad. Sci. U. S. A.* **96,** 8627–8632
13. Jamieson, T., Cook, D. N., Nibbs, R. J., Rot, A., Nixon, C., McLean, P., Alcami, A., Lira, S. A., Wiekowski, M., and Graham, G. J. (2005) *Nat. Immunol.* **6,** 403–411
14. Junqueira, L. C., Bignolas, G., and Brentani, R. R. (1979) *Histochem. J.* **11,** 447–455
15. Leers, M. P., Kolgen, W., Bjorklund, V., Bergman, T., Tribbick, G., Persson, B., Bjorklund, P., Ramaekers, F. C., Bjorklund, B., Nap, M., Jornvall, H., and Schutte, B. (1999) *J. Pathol.* **187,** 567–572
16. Moloney, W. C., McPherson, K., and Fliegelman, L. (1960) *J. Histochem. Cytochem.* **8,** 200–207
17. Yang, S. Q., and Craik, C. S. (1998) *J. Mol. Biol.* **279,** 1001–1011
18. Eggers, C. T., Wang, S. X., Fletterick, R. J., and Craik, C. S. (2001) *J. Mol. Biol.* **308,** 975–991
19. Cerf, M. E., and Raidoo, D. M. (2000) *Metab. Brain. Dis.* **15,** 315–323
20. Ciechanowicz, A., Bader, M., Wagner, J., and Ganten, D. (1993) *Biochem. Biophys. Res. Commun.* **197,** 1370–1376
21. Neth, P., Arnhold, M., Nitschko, H., and Fink, E. (2001) *Thromb. Haemost.* **85,** 1043–1047
22. Metcalfe, D. D., Baram, D., and Mekori, Y. A. (1997) *Physiol. Rev.* **77,** 1033–1079
23. Duttlinger, R., Manova, K., Chu, T. Y., Gyssler, C., Zelenetz, A. D., Bachvarova, R. F., and Besmer, P. (1993) *Development* **118,** 705–717
24. McIntyre, J. A., Neerunjun, E. D., Faulk, W. P., and Papamichail, M. (1981) *Int. Arch. Allergy Appl. Immunol.* **66,** 244–250
25. Wolters, P. J., Pham, C. T., Muilenburg, D. J., Ley, T. J., and Caughey, G. H. (2001) *J. Biol. Chem.* **276,** 18551–18556
26. Alexander, C. M., Selvarajan, S., Mudgett, J., and Werb, Z. (2001) *J. Cell*

Biol. **152,** 693–703
27. Lund, L. R., Romer, J., Thomasset, N., Solberg, H., Pyke, C., Bissell, M. J., Dano, K., and Werb, Z. (1996) *Development* **122,** 181–193
28. Mandrup, S., and Lane, M. D. (1997) *J. Biol. Chem.* **272,** 5367–5370
29. Smas, C. M., and Sul, H. S. (1995) *Biochem. J.* **309,** 697–710
30. Spiegelman, B. M., and Ginty, C. A. (1983) *Cell* **35,** 657–666
31. Strange, R., Li, F., Saurer, S., Burkhardt, A., and Friis, R. R. (1992) *Development* **115,** 49–58
32. Ichinose, A., Kisiel, W., and Fujikawa, K. (1984) *FEBS Lett.* **175,** 412–418
33. Schmaier, A. H., and McCrae, K. R. (2007) *J. Thromb. Haemost.* **5,** 2323–2329
34. Neth, P., Arnhold, M., Sidarovich, V., Bhoola, K. D., and Fink, E. (2005) *Biol. Chem.* **386,** 101–109
35. Razin, E., Ihle, J. N., Seldin, D., Mencia-Huerta, J. M., Katz, H. R., LeBlanc, P. A., Hein, A., Caulfield, J. P., Austen, K. F., and Stevens, R. L. (1984) *J. Immunol.* **132,** 1479–1486